Synthesis and Retanning Performance of a Novel Melamine Resin with Ultralow Formaldehyde Content

by
Nan Sun,[1] Ji-bo Zhou,[1] Xue-pin Liao[1,2*] and Bi Shi [1,2]
[1]*Department of Biomass and Leather Engineering, Sichuan University*
Chengdu 610065
[2]*National Engineering Research Center of Clean Technology in Leather Industry*
Chengdu 610065

Abstract

Diethanolamine, epichlorohydrin (ECH), and lysine were used to change the traditional synthesis route to address the formaldehyde emission issue of melamine resin (MR), and a novel waterborne MR retanning agent with ultralow formaldehyde content (MUF) was finally obtained. The structure of MUF was characterized by Fourier transform infrared spectroscopy, ^{13}C nuclear magnetic resonance, and X-ray photoelectron spectroscopy, and its retanning performances in wet-blue and wet-white leathers were thoroughly investigated. Results showed that the formaldehyde content of MUF was 28.05 mg/kg, which was greatly lower than that of traditional MR (3550.23/2543.45 mg/kg), and the formaldehyde contents of chrome- and TWLZ-tanned leathers retanned by MUF were only 12.68 and 8.98 mg/kg, respectively. The thickening rates of MUF-retanned leather were up to 13.40% (chrome-tanned leather) and 9.58% (TWLZ-tanned leather), and MUF showed a satisfying overall performance in retanning leather. MUF is highly promising in practical application owing to its ultralow formaldehyde content, excellent stability in aqueous solution, and satisfactory retanning behaviors.

Introduction

Melamine resin (MR) has high filling and coordination ability in the leather retanning process, but the formaldehyde emission issue has limited its further application.[1] Formaldehyde is a proven carcinogen; inhaling it may have chronic effects, such as shortened lifespan, reproductive problems, and lower fertility.[2] Many countries have set standards for formaldehyde content in leather, and this restriction is becoming increasingly stringent.[3–4]

The common approach to decreasing the formaldehyde content in MR is to reduce the molar ratio of formaldehyde/melamine in the synthesis process.[5] However, the reduction of formaldehyde dosage definitely lowers the reactivity of the synthesis process and finally causes poor retanning performances. Other attempts were also conducted, including optimizing synthesis parameters, adding formaldehyde scavengers, and replacing starting materials.[6] Even these attempts are somewhat effective to reduce the formaldehyde content of MR, but the overall retanning performances and formaldehyde content in leather hardly meet the practical requirements.[1, 6–7] Therefore, a novel MR with excellent retanning performances and ultralow formaldehyde content is still a challenge.

The traditional synthesis route should be changed to effectively solve the formaldehyde problem. Generally, the conventional synthesis route of MR includes two processes, hydroxymethylation and condensation (Figure 1), and the dosage of formaldehyde is often excess to ensure the complete reaction of melamine.[8] In the hydroxymethylation stage, formaldehyde was reacted with melamine to generate the intermediate product, methylomelamines, but this reaction is reversible (Figure 1b). Then, in the following condensation stage, the formerly generated methylomelamines will crosslink with each other and finally result in the formation of polymer resins (MR). Accordingly, formaldehyde residues in the MR have two main sources. First, a considerable amount of unreacted formaldehyde is formed in the hydroxymethylation process, the unreacted formaldehyde is the direct source of formaldehyde in MR.[9] Second, the condensation stage is usually accompanied by the formation of methylene ether bonds (Figure 1c). Methylene ether bonds are unstable; they can break in certain conditions and finally lead to formaldehyde generation (Figure 1d).[10] The breakage of methylene ether bonds is responsible for the continuous formaldehyde release of MR. Therefore, if the intermediate product of methylomelamines can be continuously consumed, the reaction extent of melamine and formaldehyde will accordingly increase, and the unreacted formaldehyde will be mostly reduced (Figures 1a–b). If the formation of methylene ether bonds can be avoided during the condensation process of methylomelamines (Figures 1c–d), the continuous formaldehyde generation and release problem of MR can also be well addressed.

*Corresponding author email: xpliao@scu.edu.cn
Manuscript received June 6, 2022, accepted for publication August 7, 2022.

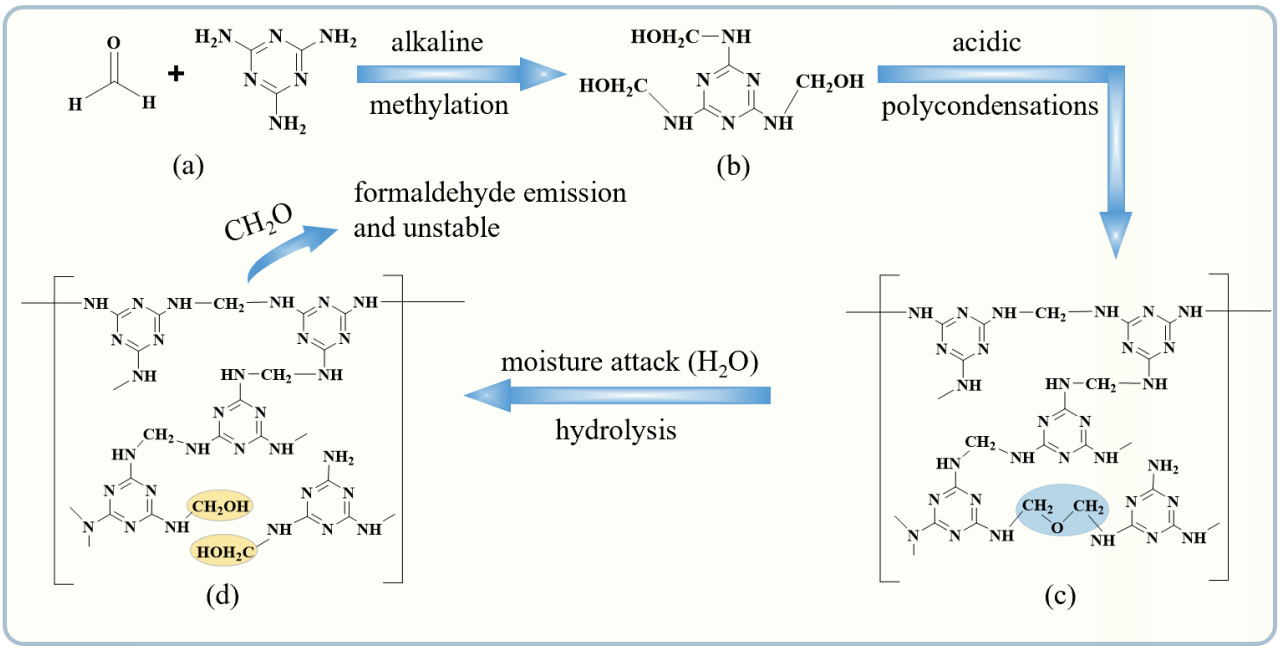

Figure 1. Synthesis process of traditional MR **(a–c)** and formaldehyde emission caused by the breakage of methylene ether bonds **(d)**.

Therefore, the aim of this study was to develop a feasible and effective method for the synthesis of ultralow-formaldehyde MR. Here, diethanolamine, formaldehyde, and melamine were first reacted to prepare triazine ring-containing polyols (TRPs, Figures 2a–b). Through this approach, the reaction of formaldehyde and melamine can be completely performed, leading to a great decrease in unreacted formaldehyde. Then, the prepared TRPs were further reacted with epichlorohydrin (ECH) to prepare the intermediate product of Chlor-containing intermediates (CCIs, Figure 2c). Finally, a condensation reaction (crosslinking) was initiated by lysine (Figure 2d), and a waterborne MR retanning agent with ultralow-formaldehyde content (MUF) was obtained.

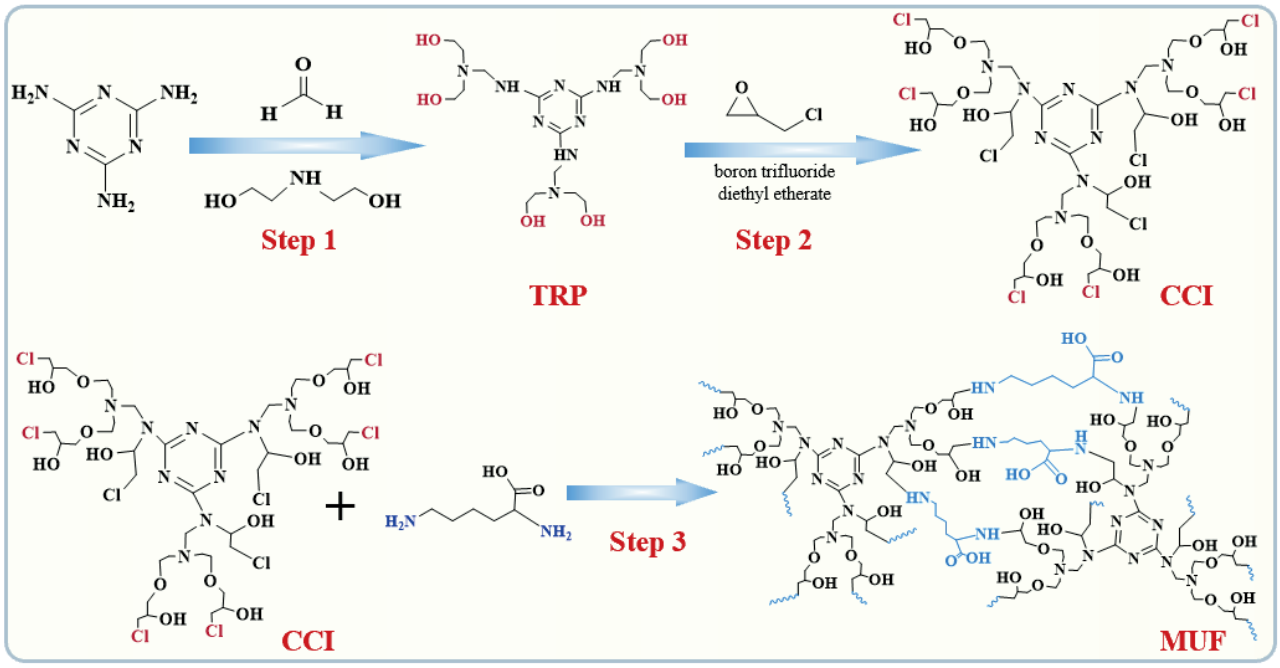

Figure 2. Schematic of the synthesis process of MUF.

Materials and Methods

Materials

Paraformaldehyde, diethanolamine, melamine, boron trifluoride diethyl etherate, acetone, sodium hydroxide and ECH were analytically pure and purchased from Chengdu Kelong Reagent Chemical Factory, China. Lysine was obtained from Shandong Usolf Chemical Technology Co., Ltd, China. Acetonitrile was chromatographically pure and purchased from Sigma-Aldrich Co., LLC, USA. Wet-blue and wet-white leathers were prepared by our laboratory. All other chemicals used for leather manufacturing were commercial grade. TWLZ, a commercial chrome-free tanning agent, was presented by Tingjiang New Materials Co., Ltd. (Sichuan, China).

MUF preparation

The MUF synthesis process is shown in Figure 2.

TRP synthesis

First, 315.42 g diethanolamine and 90 g paraformaldehyde were added into a 1000 mL three-neck round bottom flask with a mechanical stirrer. The three-neck flask was placed in an oil bath at 80°C, and the reaction was stirred for 1.5 h. Then, 126 g melamine was added to the flask for 6 h to prepare TRPs. The TRP was washed thrice with acetone and filtered to remove unreacted components, and the yield was 78.96%.

CCI preparation

The prepared TRP (24 g) and boron trifluoride diethyl etherate (0.7 g) were added to the three-neck flask and stirred for 5 min at room temperature. Thereafter, 45 g ECH was dripped into the above mixture within 30 min. Afterward, the temperature of the oil bath was increased to 60°C and held for 24 h. Finally, a clear and transparent CCI solution was obtained. The CCI was washed thrice with acetone and filtered to remove unreacted components, and the yield was 89.86%.

MUF synthesis

Lysine (8.22 g) was dissolved in 24.66 g water, and the solution was then transferred to a three-neck flask to react with 12.9 g CCI at 60°C for 2 h. Afterward, the temperature was increased to 90°C for further reaction for 2 h, and the mixture was kept in pH 9~10 conditions by 30% NaOH solution throughout the reaction. The MUF was purified by dialysis through dialysis tubing (MWCO, 500) for three days and freeze-dried.

Characterization of intermediate and final products

Fourier transform infrared (FTIR) spectroscopy analysis

TRP, CCI, and MUF were separately lyophilized, and FTIR spectroscopy (Nicolet IS10, Thermo Scientific, USA) was used to characterize their structures in the wave range of 400–4000 cm^{-1} using compressed KBr pellets. The crust leathers retanned by MUF, CMS, CML, and control sample (without retanning) were trimmed into 2 cm×2 cm pieces to be tested using FTIR spectroscopy.

Nuclear magnetic resonance (NMR) spectroscopy

The ^{13}C-NMR spectra of TRP, CCI, and MUF were recorded on a Bruker Advance II 400MHz NMR spectrometer (Bruker, Swiss). The solvent used for TRP and CCI was dimethyl sulfoxide (DMSO-d6, 99.8 atom% D) containing 0.03% (v/v) tetramethylsilane (TMS), and the solvent for MUF was deuterium oxide (D_2O, 99.8 atom% D) because of their differences in solubility.

X-ray photoelectron spectroscopy (XPS) analysis

XPS elemental surface analysis was achieved through an X-ray photoelectron spectrometer (Thermo Fisher Nexsa, USA) with a monochromator Al Kα X-ray source (1486.6 eV).

Storage stability and release of formaldehyde content during storage

The prepared products adjusted to pH 3.8/7.0 were stored at 80°C for 168 hours, which could accelerate the methylene ether bond breakage and molecular movement in the solution. During storage, the storage stability of the prepared products was assessed by observing the state of the solutions, and the formaldehyde contents were also determined by high-performance liquid chromatography (HPLC) according to ISO/TS 17226:2003. For comparison, a typical commercial liquid MR (CML) was also evaluated.

Particle size and isoelectric point (pI) analysis

The average particle size of the MUF solution (1 g/L) was determined by NanoBrook Omni (Brookhaven, USA). The pH of the MUF solution was adjusted to the pH gradient of 2–10 with 1 mol/L HNO_3 and 1 mol/L NaOH to further measure the pI of MUF. For comparison, two typical commercial melamine resins, CML and powder (CMS), were also investigated. CML is in the liquid form and has a higher degree of sulfonation, whereas CMS is in a powder form with a low degree of sulfonation.

Retanning performances of MUF

The retanning performances of MUF in wet-blue (chrome tanned) and wet-white leathers (TWLZ tanned) were investigated. The leather

Table I

Wet-blue retanning processes

Process	Chemicals	%	Duration (min)	Remarks
Rewetting	Water	250		
	Degreasing agent	0.3		
	Formic acid	0.5	60	pH≈3.2, Drain
Washing	Water	400	10	Drain
Chrome Retanning	Water	200		
	Chrome powder	4	90	
	Sodium formate	1	30	pH≈3.4
	Sodium bicarbonate	0.3	90	pH≈4.0, Drain
Neutralization	Water	200		
	Sodium formate	2	30	
	Neutralization tannins	2		
	Sodium bicarbonate	1	60	pH≈5.5, Drain
Washing	Water	400	10×2	Drain
Retanning	Water	100		
	MUF/CML/CMS	10	90	
Fatliquoring	Water	100		
	Fatliquoring agent	8	50	
	Formic acid	2	4×15	pH≈3.4
Washing	Water	400	10×3	Drain

Note: based on wet blue weight (w/w)

Table II

Wet-white retanning processes

Process	Chemicals	%	Duration (min)	Remarks
Rewetting	Water	400		
	Nonionic degreasing agent	0.5		
	Formic acid	0.3	40	
Neutralization	Water	200		
	Sodium formate	2		
	Neutralization tannins	3	30	
	Sodium bicarbonate	0.6×2	15×2+60	pH≈6.0, Drain
Washing	Water	400×2	10×2	Drain
Retanning	Water	100		
	Synthetic tanning agent	10	90	
	MUF/CML/CMS	10	120	Drain
Fatliquoring	Water	150		
	Fatliquoring agent	10	120	
	Formic acid	0.4×2	15×2	pH≈3.6
Washing	Water	200	15	Drain

Note: based on shaving leather weight (w/w)

samples were cut into halves through the backbone. The retanning processes are summarized in Tables I (wet-blue leather) and II (wet-white leather). It should be noted that TWLZ is a kind of aluminum-zirconium combination tanning agent, and the isoelectric point of TWLZ leathers is higher than that of wet blue tanned by chrome tanning agent. As a result, in the retanning process of TWLZ, the neutralization pH of TWLZ tanning is set higher than chrome tanning to maintain an appropriate gap between bath pH and TWLZ leather isoelectric point, which can avoid leather from the excessive surface combination. For comparison, the two commercial MR agents (CML and CMS) were also investigated as the control samples.

Absorption of retanning and fatliquoring agents

The effluents before and after the retanning/fatliquoring process were individually collected to measure the absorption of retanning/fatliquoring agents based on total organic carbon (TOC) concentration (Elementar, Germany). The absorption rates of the retanning agents were calculated using Equation (1):

$$\text{Absorption rates} = \frac{(T_1 - T_2)}{T_1} \times 100\% \quad (1)$$

where T_1 and T_2 are the TOC values of the bath collected at the beginning and ending of retanning/fatliquoring, respectively.

Thickening rates of retanned leather

The average thickness of the leather samples were measured by a dial thickness gauge (MingYu, China), and thickness rate (R) was calculated as follows:

$$R = \frac{(S_2 - S_1)}{S_1} \times 100\% \quad (2)$$

where S_1 and S_2 are the average thicknesses of the leather samples before and after retanning, respectively.

Physical and mechanical strength of leather

All samples were kept at 25±2°C and 65%±2% relative humidity for more than 48 h before measuring. The physical and mechanical strengths of the samples, including tensile strength, tearing strength, and elongation at break, were tested by a universal testing machine (GOTECH, China) according to ISO 3377-2: 2016 and ISO 3376: 2020.[11–12]

Determination of free formaldehyde content in leather

The free formaldehyde contents of retanned leather samples were determined by HPLC method according to ISO/TS 17226: 2018.[13]

Results and discussion

Characterization of retanning agents

FTIR analysis

The FTIR spectra of TRP, CCI, and MUF are illustrated in Figure 3a, respectively.

The strong and wide peak at 3342 cm^{-1} in the spectra of the TRPs was assigned to the stretching vibrations of hydroxyl and second amino groups, indicating the successful conjugation of hydroxymethyl groups and melamine.[14] A Mannich–type reaction occurred among diethanolamine, formaldehyde, and melamine. Due to the imino group of diethanolamine having a greater basicity than that of melamine's primary amino group, N–hydroxymethyl diethanolamine was first synthesized, and melamine was then combined to prepare TRP. Moreover, peaks at 1559 and 814 cm^{-1} were attributed to the vibration of triazine rings; the observation of these peaks in TRP is also a strong evidence of the successful reaction of melamine and formaldehyde.[15] The peak at 2945 cm^{-1} is assigned to the stretching vibration of C–H bonds from diethanolamine, which further confirms the successful reaction.[16] In the CCI spectra, the introduction of ECH can be proven by the

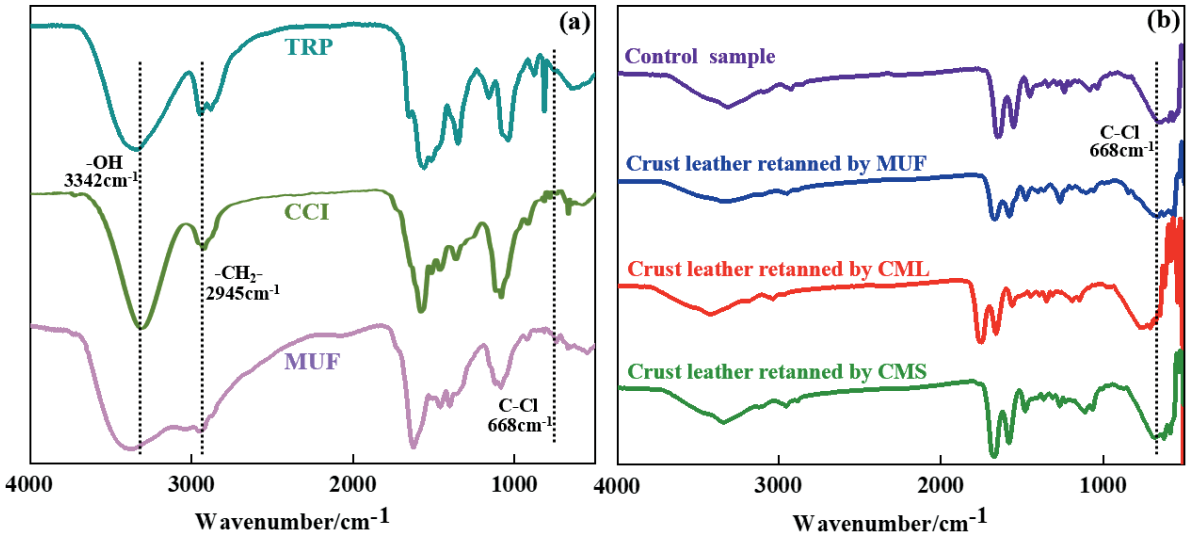

Figure 3. FTIR spectra of TRP, CCI, and MUF **(a)**; FTIR spectra of crust leather retanned by MUF, CMS, CML and control sample **(b)**.

C–Cl stretching vibration peak at 668 cm^{-1}.[17] Moreover, the weak peak at 1083 cm^{-1} was attributed to ether bonds originating from the ring-opening reactions of epoxy groups, which also suggests the successful synthesis of CCI.[18] After the introduction of lysine, the peak at 668 cm^{-1}, which was assigned to C–Cl stretching vibration, almost disappeared in the MUF spectra, indicating the occurrence of the nucleophilic substitution between the C–Cl of CCI and the $–NH_2$ of lysine. Moreover, the asymmetric and symmetric stretching vibrations of methylene from lysine can be observed at 2924 and 2853 cm^{-1}, respectively; the appearance of these peaks further proved the successful introduction of lysine.[19]

The FTIR spectra of the crust leather retanned by MUF, CMS, CML, and control sample are shown in Figure 3b. The absences of the C-Cl signal at 668 cm^{-1} in the spectra of all samples prove that there is no chloride contained in the crust leather.

NMR

^{13}C-NMR was further employed to confirm the structure of products, the results and the carbon atoms of TRP, CCI, and MUF are presented in Figures 4a–c. First, in the spectrum of TRP, signals of melamine triazine carbons can be observed at 167.47, 167.11, and 163.34 ppm, these three peaks are assigned to di-, tri-, and monosubstituted melamine, respectively.[20] The appearance of these peaks indicates the successful reaction among diethanolamine, formaldehyde, and melamine. Moreover, the peaks at 60.62 and 56.02 ppm are attributed to the two $–CH_2–$ in diethanolamine, which further confirm the success of the reaction.[21] Moreover, the peaks observed in the 58–60 ppm region are assigned to different hydroxymethyl groups, which suggests that few hydroxymethyl groups remained in TRP.[22] Interestingly, the peak at 86.58 ppm is due to formaldehyde hydration.[23] Considering that a large excess of $–NH_2$ and –NH– groups were formed in the synthesis process of TRP, the presence of this peak implies that the reaction between –CHO and $–NH_2$ groups is incomplete and will finally maintain a delicate balance. For this reason, formaldehyde is hard to consume completely during synthesis; this reason also explains why the formaldehyde content stayed at a very high level in the synthesized MR compared with that obtained in the traditional methylation–condensation process.

In the ^{13}C-NMR spectrum of CCI, the peaks of different hydroxymethyl groups at the 58–60 ppm region disappeared, and only a single peak at 163.44 ppm was found. These changes were all related to the ring-opening reaction between $–OH/–NH_2$ and epoxy groups, indicating the successful introduction of –Cl.[24] Moreover,

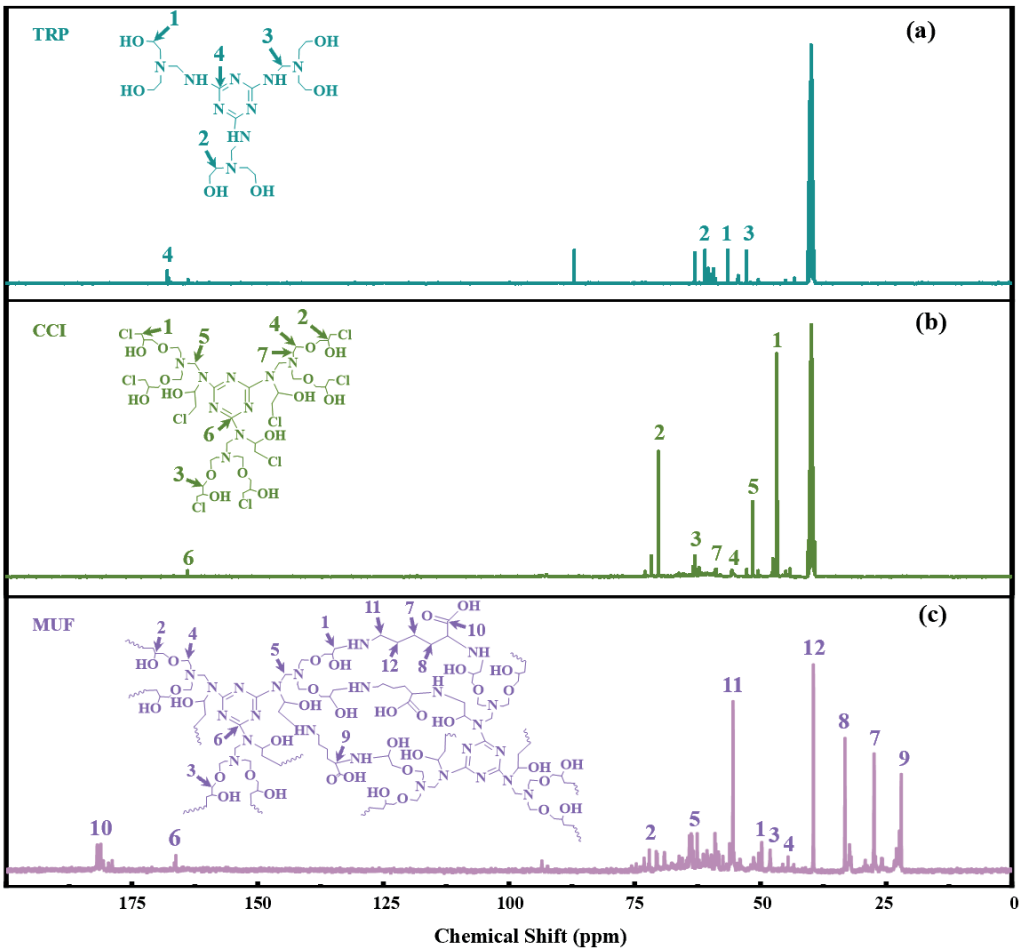

Figure 4. ^{13}C-NMR spectra of TRP **(a)**, CCI **(b)**, and MUF **(c)**.

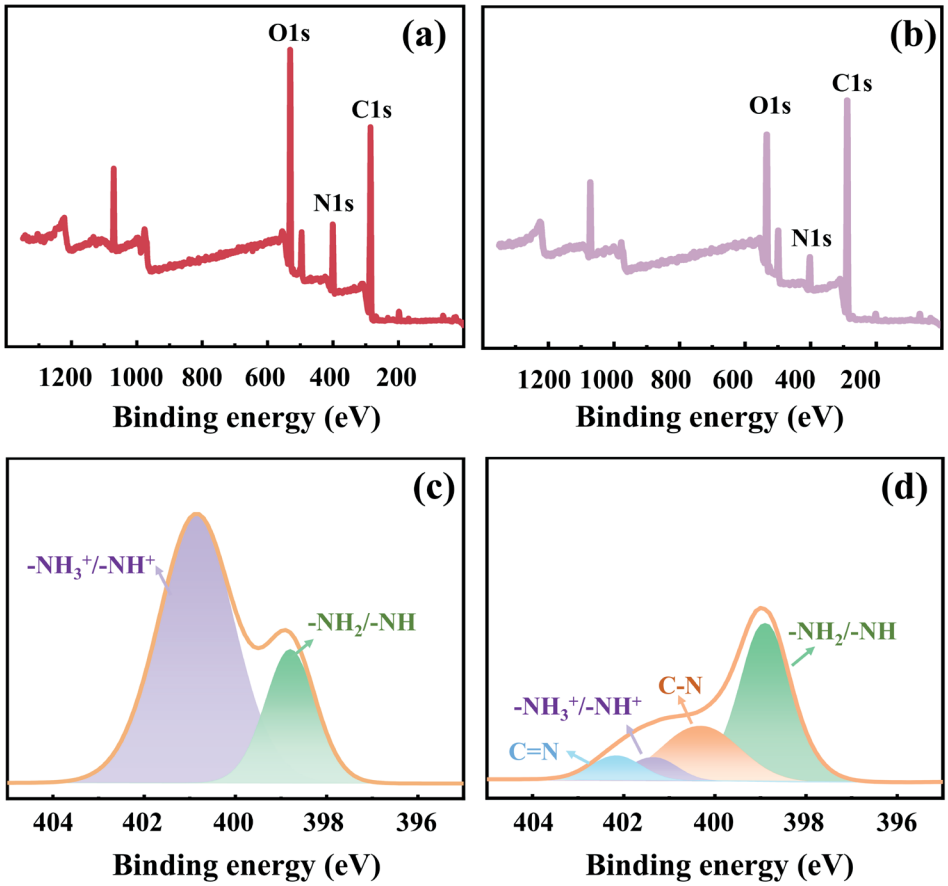

Figure 5. Survey scans of lysine **(a)** and MUF **(b)**; N 1s XPS spectra of lysine **(c)** and MUF **(d)**.

the newly appeared peaks at 46–48 ppm region in the spectra of CCI were assigned to the different types of carbon atoms that are linked to chlorine atoms. The appearances of these peaks prove the successful synthesis of CCI.[25]

The final product of MUF was obtained after the polymerization of CCI was initiated by lysine. Figure 4c shows five strong peaks at 55.44, 39.47, 33.18, 27.39, and 22.01 ppm. These peaks are attributed to the methine and methylene carbons in lysine, indicating the nucleophilic substitution reaction between $-NH_2$ in lysine and –Cl in CCI.[26] Moreover, this reaction can also be evidenced by the disappearance of peaks at 46–48 ppm, which is assigned to carbon atoms linked to chlorine atoms. In addition, many small peaks are distributed at 47–52 and 57–77 ppm. These peaks correspond to different kinds of methyl in MUF. The occurrence of these peaks is attributed to the different degrees of substitution.[27]

XPS analysis

The elemental and bond energy variations of lysine and MUF were further analyzed by XPS as shown in Figure 5. In the full XPS spectra of lysine and MUF, the absorption peaks with binding energies at 285, 400, and 531.2 eV are attributed to C 1s, N 1s, and O 1s, respectively, which are the major elemental compositions of lysine and MUF. The N spectrum of lysine in Figure 5c has two main peaks at 398.85 and 400.87 eV, corresponding to $-NH_2$ in the lysine molecule and ionic states $-NH_3^+$ and $-NH^+$ formed between the lysine molecules, respectively.[28] After reaction with CCI, the N spectrum of MUF (Figure 5d) shows four peaks at 399.06, 400.29, 401.31, and 402.16 eV, which are attributed to $-NH_2$/–NH, C–N, $-NH_3^+$/$-NH^+$, and C=N in MUF, respectively. Moreover, compared to Figure 5c, Figure 5d shows an obvious decrease in the intensity of NH_3^+/NH^+, further indicating that chlorine from CCI has successfully reacted with the deprotonated form of lysine.[29–30]

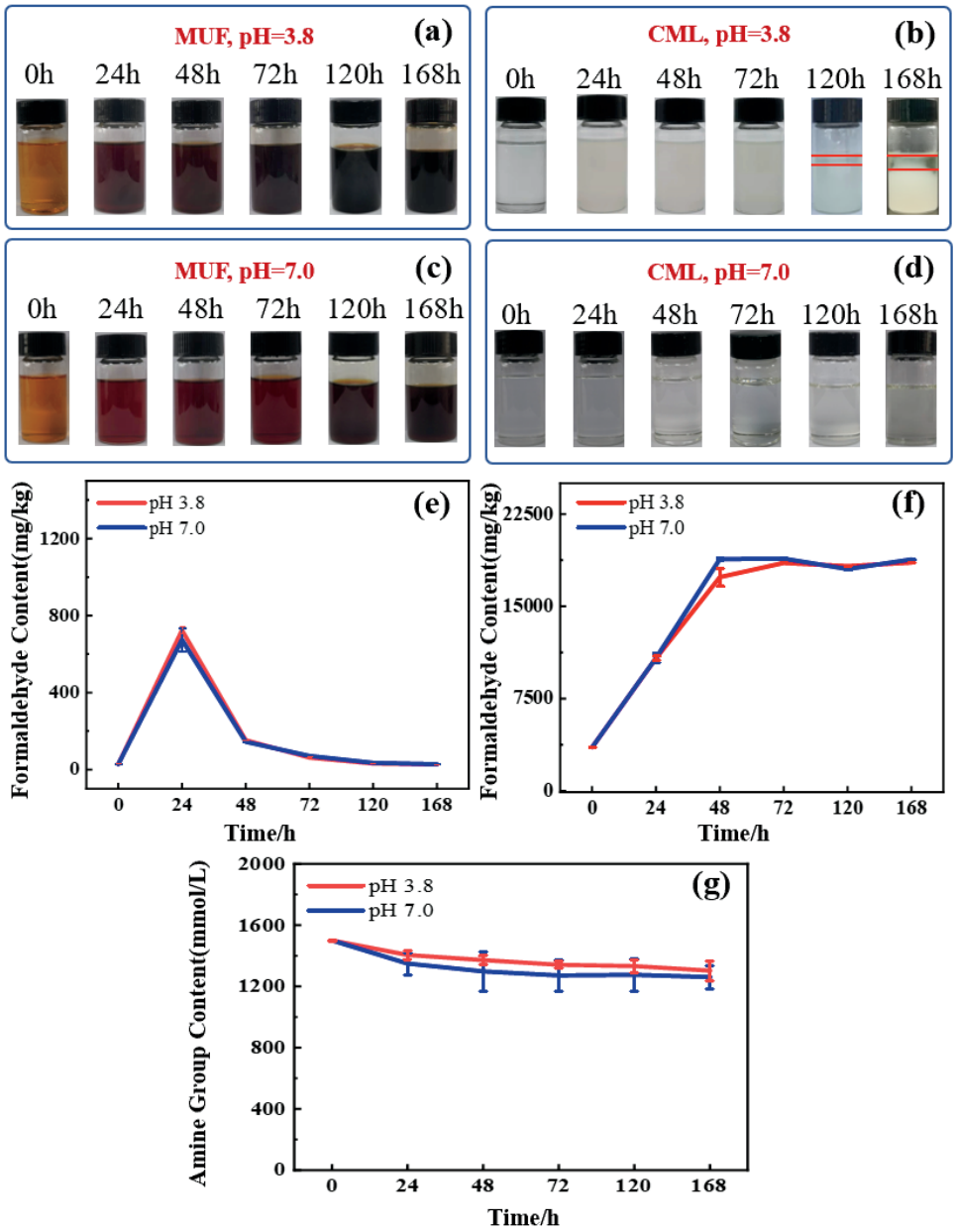

Figure 6. Stability of MUF at pH 3.8 **(a)**, CML at pH 3.8 **(b)**, MUF at pH 7.0 **(c)**, and CML at pH 7.0 **(d)**; formaldehyde content evolutions of MUF **(e)** and CML **(f)** during observation; amine group content evolutions of MUF **(g)** during observation.

Storage stability and formaldehyde determination of retanning agents

The storage stability of liquid MUF and CML at pH 3.8 and 7.0 were exhibited in Figures 6a–d. The alkaline conditions were not evaluated because the leather manufacturing processes were mostly conducted in acidic conditions. Storage stability is an important indicator of hydroxymethyl contents. Hydroxymethyl groups have high activity; they can condense with each other during storage and finally precipitate out.[31] Precipitation was observed in CML at pH 3.8 after being placed at 80°C for 120 h, whereas MUF was stable during observations. CML was synthesized by the traditional hydroxymethylation–condensation process, and large amounts of residual hydroxymethyl groups were found in the product. The residual hydroxymethyl groups will be further condensed and lead to an unstable state. However, hydroxymethyl groups were mostly consumed in MUF and thus show high stability even at an extremely low pH. Considering its very low content of hydroxymethyl groups, MUF should have ultralow-formaldehyde emission.

It can be observed in Figures 6a and 6c that the color of MUF became darker during storage testing. MUF is rich in hydroxyl groups, and some of them were oxidized to aldehydes and ketones

during storage at 80°C. These aldehydes and ketones interacted with free amino groups to cause the Maillard reaction, and finally resulted in an increase of the color intensity.[32] Therefore, MUF is advised against storing in high-temperature environments.

The continuous release of free formaldehyde in MR is greatly related with the amount of methylene ether bonds. Figures 6e–f shows the formaldehyde content evolutions of CML and MUF during observation. The formaldehyde content of CML showed an increasing trend with time at different pH and tended to be stable after 72 h. This phenomenon can be attributed to the breakage of methylene ether bonds in CML, which can lead to the release of free formaldehyde. Afterward, the methylene ether bonds in CML were mostly consumed, and its formaldehyde content tended to stabilize. After 168 h, the formaldehyde content of CML were 18555.99 and 18813.90 mg/kg at pH 3.8 and 7.0, respectively. The formaldehyde content of MUF initially increased and then decreased. In the first step of MUF preparation, a small amount of methylene ether bonds were generated as shown in the ^{13}C NMR analysis, which will breakdown, and release formaldehyde at a higher temperature. However, the maximum formaldehyde content of MUF was only 724.02 mg/kg, which was much lower than that of CML. The decreasing stage can be attributed to the presence of large amounts of $–NH_2$/–NH in MUF. These groups can react with the released formaldehyde. After 168 h, the formaldehyde content in MUF greatly decreased to 26.14 and 28.23 mg/kg at pH 3.8 and 7.0, respectively, indicating the great advantage of the proposed new synthesis method for MUF. The amine group content changes of MUF over the course of storage were presented in Figure 6g. Before 72 hours, the amine group content was significantly decreased at pH 3.8 and 7.0, but it was almost unchanged after 72 hours, providing strong support for the reaction between $–NH_2$/–NH and the released formaldehyde.

Particle size and zeta potential

The average particle sizes and zeta potentials of MUF, CML, and CMS are summarized in Figure 7. The average particle size of MUF was 392 nm, which was slightly lower than those of CMS (593 mm) and CML (587 nm). The particle size and size distribution of retanning agents greatly affect their retanning performance.[33] A particle size that is too large may result in insufficient leather penetration, whereas a small particle size may decrease the filling performance. According to literature, the diameter of collagen fibers in leather is approximately 0.5–20 μm, and the average spacing between fibers is 2.5 μm.[34] Therefore, MUF can easily penetrate leather and fill collagen fibers well.

Apart from particle size, the charges of retanning agents will also affect their penetration and uptake in leather. Chrome-tanned leather is positively charged, and retanning agents are usually designed as an anionic type to facilitate their absorption.[35] In chromium-free tanned leather, the charge mismatch between wet white and retanning agents will result in the poor quality of the finished leather. Fortunately, amphoteric agents are promising in solving the charge mismatch problem owing to their pH-responsive function.[36] As illustrated in Figure 7b, the pI values of MUF and CMS were 5.08 and 4.56, respectively. Lysine is a basic amino acid with two amino groups, which could increase the pI of MUF and is beneficial for the absorption of anionic retanning agents. However, CML is in the anionic state at pH 1–10 because of its high sulfonation degree.

Retanning performances of MUF

Absorption rates of retanning and fatliquoring agents

The absorption rates of retanning and fatliquoring agents were determined by collecting the bath at the beginning and end of the retanning and fatliquoring processes. The results are shown in

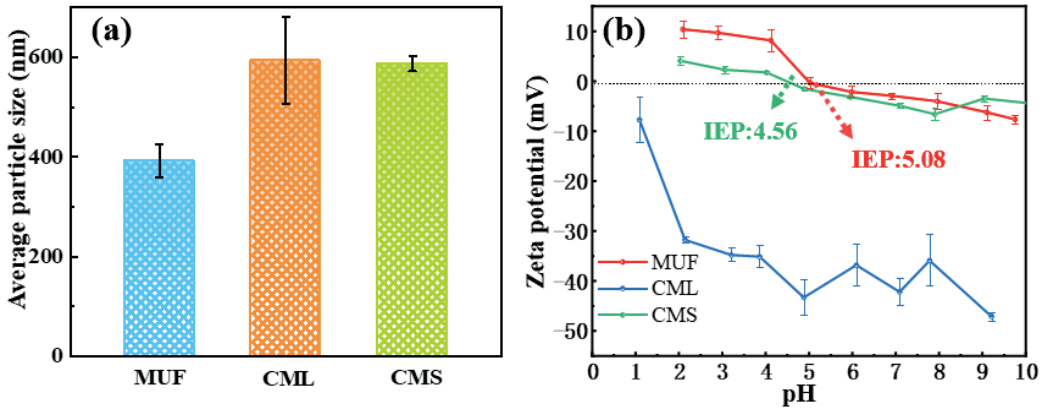

Figure 7. Average particle sizes **(a)** and zeta potentials **(b)** of MUF, CML, and CMS.

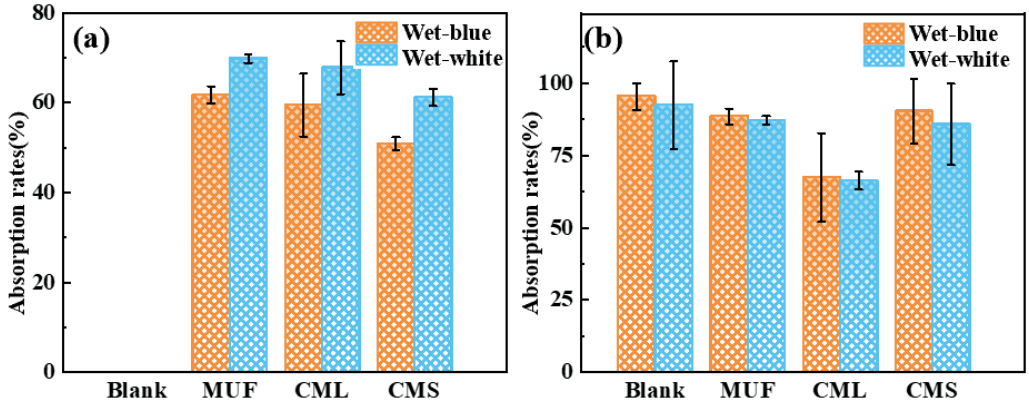

Figure 8. Absorption rates of retanning **(a)** and fatliquoring agents **(b)**.

Figure 8. MUF exhibited a higher absorption rate than CML and CMS (Figure 8a). The absorption rate of CMS was the lowest in the chrome-tanned and chrome-free leather because of the poor solubility of CMS. Notably, compared with commercial MRs, the leather samples retanned by MUF manifested a high absorption rate by the fatliquoring agents in wet-blue and wet-white leathers (Figure 8b). The pH of the retanning process was about 5.5. MUF was in an anionic state in this condition, and the electrostatic attraction between MUF and collagen fiber is beneficial for its combination.[37] Moreover, in the following fatliquoring stage, the final pH of the bath was controlled at 3.8, at which MUF was in a cationic state and can further promote the absorption of anionic fatliquoring agents. This result further proved the superiority of amphoteric retanning agents in leather manufacturing.

Physical and mechanical strengths

The physical and mechanical strengths of the leather samples retanned by MUF, CMS, and CML, including thickening rate, tensile strength, tear strength, and elongation at break, were thoroughly determined. As shown in Figure 9, the thickening rates of the wet-blue and wet-white leathers retanned by MUF were higher than those retanned by CMS but were lower than those retanned by CML (Figure 9a). The tensile strengths, tear strengths, and elongation at break of the leather samples retanned

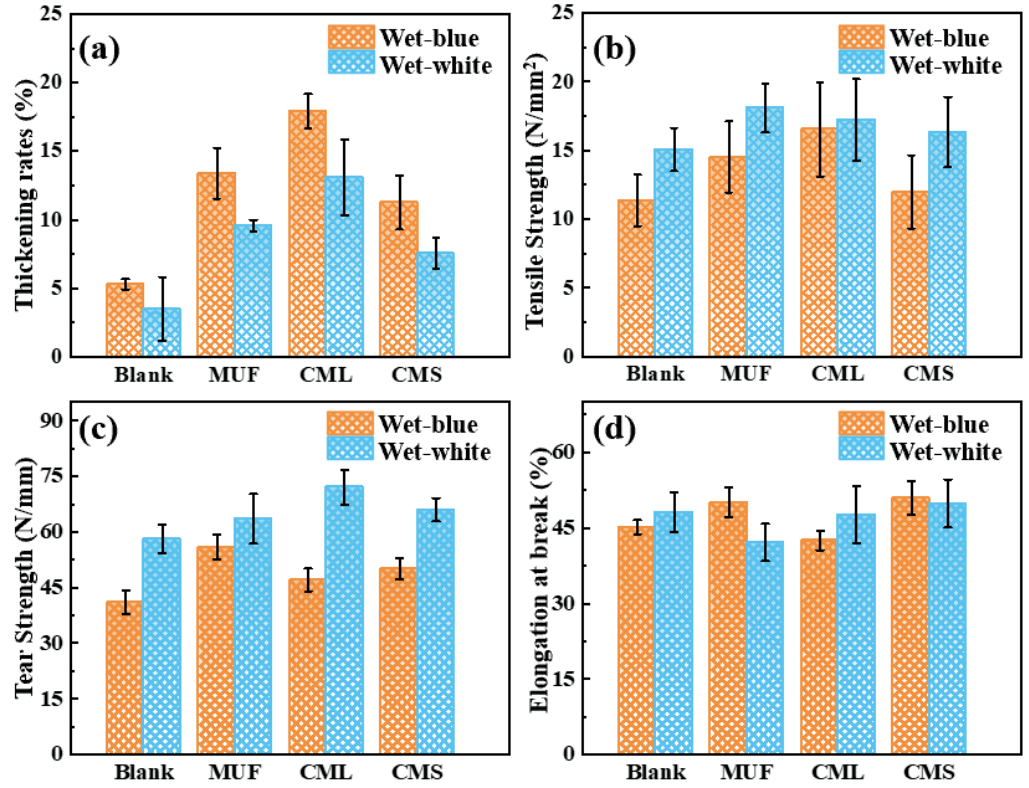

Figure 9. Physical and mechanical strengths of leather samples retanned by MUF, CML, and CMS: thickening rates **(a)**, tensile strength **(b)**, tear strength **(c)**, and elongation at break **(d)**.

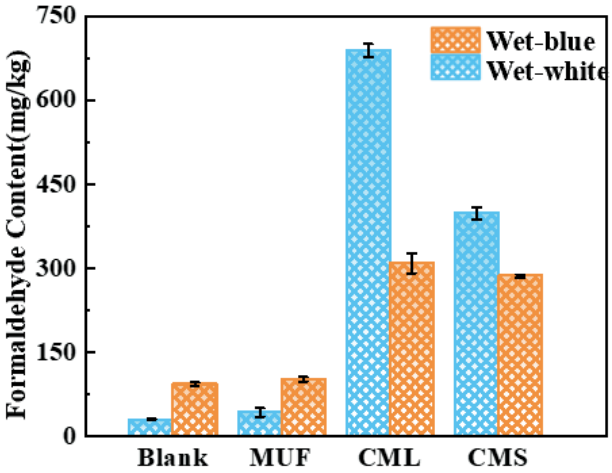

Figure 10. Formaldehyde contents of leather samples retanned by MUF, CML, and CMS.

by MUF were comparable to those retanned by CML and CMS; overall, MUF and CML showed better performances than CMS (Figures 9b–d). Compared with the blank, the tensile and tear strengths of the leathers retanned by MR were all enhanced (Figures 9b–c). In general, the retanning process often refers to the generation of cross-linked bonds between the retanning agents and collagen polypeptide chains. These bonds can improve the physical and mechanical strengths of the leather. In the molecular structures of MUF, –OH, $–NH_2$, and –COOH groups may form multipoint cross-linking with collagen fibers and finally lead to the improvement of mechanical strength.

Determination of free formaldehyde in leather

Figure 10 shows the formaldehyde content of the leather samples retanned by different agents. The formaldehyde content in blank blue and white leather samples without retanning were 29.27 and 92.49 mg/kg, respectively, which possibly originated from the pretreatment and tanning process. After the samples were retanned by commercial MR retanning agents (CML and CMS), the formaldehyde content of wet-white and wet-blue leathers reached as high as 688.17/308.74 and 398.05/286.12 mg/kg, respectively. Compared with the blank samples, the formaldehyde contents of the wet-white and wet-blue leather samples retanned by MUF only increased by 12.68 and 8.98 mg/kg, respectively. These facts suggest that MUF application did not remarkably increase the formaldehyde content of leather. Economic analysis was conducted and the cost of UF was estimated within $1.00/kg, which is comparable with commercial retanning agents, showing a promising application potential.

Conclusion

A new synthesis method was proposed in this study to solve the formaldehyde issue in MR, and an ultralow-formaldehyde MR retanning agent, MUF, was prepared. In the synthesis process, the introduction of diethanolamine changed the route of hydroxymethyl reaction and greatly reduced the residue of formaldehyde, and ECH changed the state of the intermediate product compared with the traditional approach. Importantly, the polymerization initiated by lysine extremely reduced the formation of methylene ether bonds, which fundamentally solved the continuous release of formaldehyde during storage and application. MUF could be applied in the retanning process of chrome-tanned leather and TWLZ (chrome-free)-tanned leather and exhibited outstanding retanning performances. Therefore, this novel MR preparation strategy is successful, and the obtained product has a good potential application prospect.

Acknowledgment

This project is financially supported by the National Key R & D Program of China (2017YFB0308500). The authors thank Dr. Zhong-hui Wang of the College of Biomass Science and Engineering, Sichuan University for experimental assistance.

Reference

1. Yu, Y., Wang, H., Wang, Y. N., Zhou, J. F., Shi, B.; Construction of a chrome-free tanning system based on highly-oxidized starch–zirconium complexes. *JALCA*, **117**, 87–95, 2022.
2. Kolisnyk, A., Chugai, A., Chernyakova, O., Kuzmina, V.; Methodical bases for taking into account the impact of air pollution on the population lifespan (on the example of the city of Odessa, Ukraine). *Ecol. Eng. Environ. Technol.* **23**, 40–46, 2022.
3. Kristak, L., Antov, P., Bekhta, P., Lubis, M. A., Iswanto, A. H., Reh, R., Sedliacik, J., Savov, V., Taghiyari, H. R., Papadopoulos, A. N.; Recent progress in ultra-low formaldehyde emitting adhesive systems and formaldehyde scavengers in wood-based panels: a review. *Wood Mater. Sci. Eng.* **17,** 1–20, 2022.
4. Peng, L. Q., Long, W. J., Zhang, W. H., Shi, B.; Leaching toxicity and ecotoxicity of tanned leather waste during production phase. *Process Saf. Environ. Prot.* **161,** 201–209, 2022.
5. Yang, M. L., Rosentrater, K. A.; Life cycle assessment of urea-formaldehyde adhesive and phenol-formaldehyde adhesives. *Environ. Processes*, **7,** 553–561, 2020.
6. Wang, Y. S., Sun, X. L., Han, Q. X., James, T. D., Wang, X. C.; Highly sensitive and selective water-soluble fluorescent probe for the detection of formaldehyde in leather products. *Dyes Pigm.* **188,** 109175, 2021.
7. Dorieh, A., Pour, M. F., Movahed, S. G., Pizza, A., Selakjani, P. P., Kiamahalleh, M. V., Hatefnia, H., Shahavi, M. H., Aghaei, R.; A review of recent progress in melamine-formaldehyde resin based nanocomposites as coating materials. *Prog. Org. Coat.* **165,** 106768, 2022.
8. Seidl, R., Weiss, S., Zikulnig-Rusch, E. M., Kandelbauer, A.; Response surface optimization for improving the processing behavior of melamine formaldehyde impregnation resins. *J. Appl. Polym. Sci.* **138,** 50181, 2021.
9. Yi, Y. D., Ding, W., Wang, Y. N., Shi, B.; Determination of free formaldehyde in leather chemicals. *JALCA*, **114,** 382–390, 2019.
10. Sabeti Meybod, J., Ostad Movahed, S.; The effects of several parameters on the storage stability of the melamine-formaldehyde (MF) polymers by using a traditional design of experiment (DOE) software. *J. Adhes. Sci. Technol.* **34**, 1705–1719, 2020.
11. IUP 6.; Measurement of tensile strength and percentage elongation. *JSLTC*, **84,** 317–321, 2000.
12. IUP 8.; Measurement of tear load—double edge tear. *JSLTC*, **84,** 327–329, 2000.
13. ISO 17226-1:2018 Leather - chemical determination of formaldehyde content - part 1: method using high performance liquid chromatography (second edition).
14. Zhou, J. B., Zhou, J. F., Li, P. L., Liao, X. P., Shi, B.; Preparation of formaldehyde-free melamine resin using furfural as condensation agent and its retanning performances investigation. *JALCA*, **113,** 198–206, 2018.
15. Huang, Y. L., Li, W., Xu, Y. W., Ding, M., Ding, J., Zhang, Y., Wang, Y. H., Chen, S. Y., Jin, Y. D., Xia, C. Q.; Rapid iodine adsorption from vapor phase and solution by a nitrogen-rich covalent piperazine–triazine-based polymer. *New J. Chem.* **45,** 5363–5370, 2021.
16. Zhang, X. P., Duan, Z. K., Zhao, Y. L., Wu, Y. Y., Qiu, T., Shi, X. L.; Direct determination of diethanolamine in high salinity dehydrogenation reaction solutions by ion chromatography (IC). *Anal. Lett.* **55,** 57–67, 2022.
17. Satheeshkumar, C., Jung, B. J., Jang, H., Lee, W., Seo, M.; Surface modification of parylene C film via buchwald–hartwig amination for organic solvent-compatible and flexible microfluidic channel bonding. *Macromol. Rapid Commun.* **42,** 2000520, 2021.
18. Demiral, İ., Samdan, C., Demiral, H.; Enrichment of the surface functional groups of activated carbon by modification method. *Surf. Interfaces*, **22,** 100873, 2021.
19. Yang, X., Wang, B. L., Sha, D., Liu, Y. G., Xu, J. D., Shi, K., Yu, C., Ji, X. L.; Injectable and antibacterial ε-poly (L-lysine)-modified poly (vinyl alcohol)/chitosan/AgNPs hydrogels as wound healing dressings. *Polymer*, **212,** 123155, 2021.
20. He, F., Wang, M., Luo, L., Wang, Z. X., Peng, S. Q., Li, Y. X.; Directional modulation of triazine and heptazine based carbon nitride for efficient photocatalytic H_2 evolution. *Appl. Surf. Sci.* **562,** 150103, 2021.
21 García-Abuín, A., Gomez-Díaz, D., Lopez, A. B., Navaza, J. M., Rumbo, A.; NMR characterization of carbon dioxide chemical absorption with monoethanolamine, diethanolamine, and triethanolamine. *Ind. Eng. Chem. Res.* **52,** 13432–13438, 2013.
22. Ruda, A., Widmalm, G., Wohlert, J.; O-Methylation in Carbohydrates: An NMR and MD simulation study with application to methylcellulose. *J. Phys. Chem. B*, **125,** 11967–11979, 2021.
23. Panangama, L., Pizzi, A.; A ^{13}C-NMR analysis method for MUF and MF resin strength and formaldehyde emission. *J. Appl. Polym. Sci.* **59,** 2055–2068, 1996.
24. Tohmura, S. I., Inoue, A., Sahari, S. A.; Influence of the melamine content in melamine-urea-formaldehyde resins on formaldehyde emission and cured resin structure. *J. Wood Sci.* **47,** 451–457, 2001.
25. Berger, S., Bock, W., Frenking, G., Jonas, G., Mueller, F.; NMR data of methyltitanium trichloride and related organometallic compounds. A combined experimental and theoretical study of Me_nXCl_{4-n} (n = 0–4; X = C, Si, Sn, Pb, Ti). *J. Am. Chem. Soc.* **117,** 3820–3829, 1995.
26. Sheveleva, N. N., Markelov, D. A., Vovk, M. A., Mikhailova, M. E., Tarasenko, I. I., Tolstoy, P. M., Neelov, L. M., Lähderanta, E.; Lysine-based dendrimer with double arginine residues. *RSC Adv.* **9,** 18018–18026, 2019.
27. Busico, V., Cipullo, R., Monaco, G., Vacatello, M., Segre, A. L.; Full assignment of the ^{13}C-NMR spectra of regioregular polypropylenes: methyl and methylene region. *Macromolecules*, **30,** 6251–6263, 1997.
28. Liu, Z. H., Wang, Q. M., Lü, Q. F.; L-lysine functionalized $Ti_3C_2T_x$ coated polyurethane sponge for high-throughput oil–water separation. *Colloids Surf. A Physicochem. Eng. Asp.* **640,** 128396, 2022.

29. Lu, F. F., Dong, A. Q., Ding, G. J., Xu, K., Li, J. M., You, L. J.; Magnetic porous polymer composite for high performance adsorption of acid red 18 based on melamine resin and chitosan. *J. Mol. Liq*. **294,** 111515, 2019.
30. Guo, X. J., Gao, G., Remón, J., Ma, Y., Jiang, Z. C., Shi, B., Tsang, D. C.; Selective hydrogenation of vanillin to vanillyl alcohol over Pd, Pt, and Au catalysts supported on an advanced nitrogen-containing carbon material produced from food waste. *Chem. Eng. J.* **440,** 135885, 2022.
31. Gao, D. G., Wang, P. P., Shi, J. B., Li, F., Li, W. B., Lü, B., Ma, J. Z.; A green chemistry approach to leather tanning process: cage-like octa (aminosilsesquioxane) combined with tetrakis (hydroxymethyl) phosphonium sulfate. *J. Clean. Prod*. **229,** 1102–1111, 2019.
32. Meng, X. Y., Li T. T., Song T, Chen, C., Venkitasamy, C., Pan, Z. L., Zhang, H. E.; Solubility, structural properties, and immunomodulatory activities of rice dreg protein modified with sodium alginate under microwave heating. *Food Sci. Nutr.* **7**, 2556-2564, 2019.
33. Huang, W. L., Song, Y., Yu, Y., Wang, Y. N., Shi, B.; Interaction between retanning agents and wet white tanned by a novel bimetal complex tanning agent. *J. Leather Sci. Eng.* **2,** 8, 2020.
34. Wang, X. C., Lan, X. M., Zhu, X., Sun, S. W.; Preparation of a ricinoleic acid modified amphoteric polyurethane for leather cleaner and simplifying production. *J. Clean. Prod*. **330,** 129877, 2022.
35. Wang, X. C., Sun, S. W., Zhu, X., Guo, P. Y., Liu, X. H., Liu, C. L., Li, M.; Application of amphoteric polymers in the process of leather post-tanning. *J. Leather Sci. Eng.* **3,** 9, 2021.
36. Li, Q. J., Yi, Y. D., Wang, Y. N., Li, J., Shi, B.; Effect of cationic monomer structure on the aggregation behavior of amphoteric acrylic polymer around isoelectric point. *J. Leather Sci. Eng.* **4,** 4, 2022.
37. Yu, Y., Sun, Q. Y., Zeng, Y. H., Lin, Y. R., Wang, Y. N., Shi, B.; Diagnosing the environmental impacts of typical fatliquors in leather manufacture from life cycle assessment perspective. *J. Leather Sci. Eng.* **4,** 6, 2022.